Synthesis and Characterization of Bismuth Zinc Niobate Pyrochlore Nanopowders

Sonia Maria Zanetti[a]*, Sandra Andréia da Silva*[b]

[a]*Laboratório Associado de Sensores e Materiais, Instituto Nacional de Pesquisas Espaciais,
Av. dos Astronautas, 1758, Jardim da Granja, 12227-010 São José dos Campos - SP, Brazil*
[b]*Departamento de Química, Instituto Tecnológico de Aeronáutica,
Praça Marechal Eduardo Gomes, 50, Vila das Acácias,
12228-900 São José dos Campos - SP, Brazil*

Bismuth zinc niobate pyrochlores $Bi_{1.5}ZnNb_{1.5}O_7$ (α-BZN), and $Bi_2(Zn_{1/3}Nb_{2/3})_2O_7$ (β-BZN) have been synthesized by chemical method based on the polymeric precursors. The pyrochlore phase was investigated by differential scanning calorimetry, infrared spectroscopy, and X ray diffraction. Powder and sintered pellets morphology was examined by scanning electron microscopy. The study of α-BZN phase formation reveals that, at 500 °C, the pyrochlore phase was already present while a single-phased nanopowder was obtained after calcination at 700 °C. The crystallization mechanism of the β-BZN is quite different, occurring through the crystallization of α-BZN and $BiNbO_4$ intermediary phases. Both compositions yielded soft agglomerated powders. α-BZN pellets, sintered at 800 °C for 2 hours, presented a relative density of 97.3% while those of β-BZN, sintered at 900 °C for 2 hours, reached only 91.8%. Dielectric constant and dielectric loss, measured at 1 MHz, were 150 and 4 x 10^{-4} for α-BZN, and 97 and 8 x 10^{-4} for β-BZN.

Keywords: *Pechini, microwave dielectrics, Bi_2O_3-ZnO-Nb_2O_5, powder, chemical method*

1. Introduction

Recently, intensive research has been focused on dielectric ceramics, which are commercially important as enabling materials for resonators, filters, and other key components in microwave communication systems. For these applications, the ceramics have to present the required set of properties, such as a high dielectric constant, a low dielectric loss (conversion of signal to heat, which broadens the signal), and a temperature-stable resonant frequency and/or a temperature stable capacitance[1].

Several systems have been studied like ZrO-TiO$_2$ [2], BaO-ZnO-Ta$_2$O$_5$ [3], (Ba,Sr)TiO$_3$ [4], among others. The main characteristic of these systems is the high temperature required for densification, which is a drawback for their use as multilayer capacitors co-fired with metal electrodes[5]. The cheapest and most convenient electrode has been silver which requires temperatures lower than 900 °C in the co-firing process. Considering these difficulties, alternative systems have been searched to match the dielectric properties and lower temperatures.

Pyrochlore and pyrochlore-related compounds occurring in the Bi_2O_3-ZnO-Nb_2O_5 system exhibit high dielectric constants (ϵ), relatively low dielectric losses, and compositionally tunable temperature coefficients of capacitance (TCC). These properties, allied to the low sintering temperatures (less than 950 °C), make these compounds attractive candidates for capacitor and high-frequency filter applications in multilayer structures co-fired with metal electrodes[6].

The general formula of stoichiometric pyrochlores is $A_2B_2O_7$. The structure is composed of two different types of cation coordination polyhedra where the A-site positions, eight-fold coordination, are typically occupied by larger cations, while the B-site positions, six-fold coordination, are occupied by smaller sized ones[7]. The structural formula is often written as $B_2O_6 \bullet A_2O'$, which emphasizes that the arrangement consists of a three dimensional network of octahedra (B_2O_6) linked with the A_2O' tetrahedra in the interstices.

There are two basic phases of the BZN system: cubic-pyrochlore-structure with the base composition $(Bi_{1.5}Zn_{0.5})(Zn_{0.5}Nb_{1.5})O_7$ (α-phase) and low-symmetry-structure with the base composition $Bi_2(Zn_{1/3}Nb_{2/3})_2O_7$ (β-phase). Their electrical properties are quite different for each phase (TCC is about –400 ppm/°C for the α-phase and +200 ppm/°C for the β-phase), which is an attractive feature in tunable temperature coefficient of capacitance devices[8].

BZN-based dielectrics ceramics have been systematically prepared by solid state reaction, which is known to yield large sized particles and local chemical heterogeneity. Commonly, this route can lead to multiphase powders[9-12].

Alternatively, chemical methods have been employed to achieve smaller sized particles with chemical homogeneity. Nanocrystalline materials obtained by the solution-based chemical methods are normally chemically homogeneous, with a narrow size distribution of particles, and lead to low crystallization and sintering temperatures. It is expected that ceramics derived from chemically prepared BZN nanopowders exhibit phase purity, low sintering temperatures, and homogeneous microstructure[13].

The goal of this work is to achieve chemically homogeneous BZN nanopowders (α and β phases) employing the polymeric precursors (PP) method (based on the Pechini[14] process), that has been successfully used for the synthesis of several complex oxides[15-17], and consists of the chelation of metallic cations by citric acid and a posterior polymerization by ethylene glycol. This method is cost effective due to the possibility of using common reagents instead of alkoxides. Moreover, the synthesis is carried out in aqueous solution, requiring no special atmosphere.

*e-mail: zanetti@las.inpe.br

2. Experimental

2.1. Synthesis

The starting reagents were bismuth oxide, Bi_2O_3 (99.99%, Aldrich), zinc acetate dihydrate, $C_4H_6O_4Zn.2H_2O$ (99.5%, Carlo Erba), and niobium ammonium oxalate $NH_4H_2[NbO-(C_2O_4)_3].3H_2O$ (99.5%, CBMM, Araxá, Brazil). The first step involved dissolving niobium ammonium oxalate in water and precipitating $Nb(OH)_5$ by adding NH_4OH. After filtration, the niobium hydroxide was dissolved in a citric acid (CA) aqueous solution to form niobium citrate (molar ratio CA/Nb = 3). The Nb content was gravimetrically determined as Nb_2O_5. Stoichiometric amounts of zinc acetate dihydrate, as salt, and Bi_2O_3, dissolved in an aqueous nitric acid solution, were added to niobium citrate solution heated at 60 °C to form a (Zn, Nb, Bi) complex precursor. Citric acid was added to maintain the molar ratio CA/metal = 3). The solution was kept under stirring at 60 °C and its pH was adjusted to 8-9 with ethylenediamine, resulting in a clear pale yellow solution. Ethylene glycol was added to this solution to promote polymerization of the mixed citrate, the citric acid/ethylene glycol ratio (CA/EG, mass ratio) was 60/40.

The resin was kept on a hot plate until a viscous gel was obtained and subsequently submitted to a thermal treatment at 300 °C for 4 hours in a furnace yielding a soft black powder. Portions of this black powder were heat treated for 2 hours at temperatures from 400 to 900 °C.

2.2. Characterization

The thermal decomposition of BZN precursors (powder treated at 300 °C for 4 hours) was studied using differential scanning calorimetry (DSC) (NETZSCH, STA404), at a heating rate of 10 °C/min, under air flux. Crystalline phases were determined by X ray diffraction (XRD) using a spectrometer PHILIPS PW1380, operating with the Cu$K\alpha$ radiation. The Fourier transformed infrared (FTIR) spectra in the range 400-4000 cm^{-1} were recorded on a NICOLET-MAGMA 760 spectrometer in the transmission mode (KBr method) with a resolution of 4 cm^{-1}. Raman spectra in the range 100-1000 nm were collected on a BRUKER spectrometer (FRA-106/S), using the 1064-nm excitation line of Nd-YAG Laser. The data was collected keeping the power at 60 mW, 100 scans and 4 cm^{-1} resolution.

Mean particle size and particle size distribution of samples treated at 700 °C for 2 hours were determined from the surface area values, measured by N_2 adsorption/desorption isotherms BET (MICRO-MERITICS 2000), and low angle laser light scattering – LALLS (MASTERSIZER 2000), respectively. Scanning electron microscopy (SEM) JEOL 6400 and transmission electron microscopy (TEM) PHILIPS CM200 were used to observe the morphology of powders treated at different temperatures.

Dilatometric measurements were performed using NETZSCH (DIL 402) at a heating rate of 10 °C/min for powders treated at 700 °C for 2 hours. Pellets of 12 mm in diameter and 2.0 mm in thickness were pressed and sintered at temperatures ranging from 800 to 1000 °C for 2 hours in air. The apparent density was measured by the Archimedes method and pellets microstructure evolution was examined by SEM. Electric measurements at room temperature were carried out using an impedance analyzer (HP4192A).

3. Results and Discussions

Figure 1 shows the DSC curves of the BZN powders previously treated at 400 °C for 2 hours. The DSC result reveals exothermic peaks centered at 500 and 538 °C for α-BZN and β-BZN, respectively, which correspond to the elimination of the organic material. Due to the high organic material content still present (weight loss higher than 65%, not shown here), it was not possible to observe the crystal-

lization of the pyrochlore phases, except for a small peak centered at 580 °C for the α-BZN composition, which may correspond to the crystallization of the cubic phase.

The crystalline phase evolution process for the α-BZN pyrochlore was followed by XRD, as shown in Figure 2. At 400 °C the presence

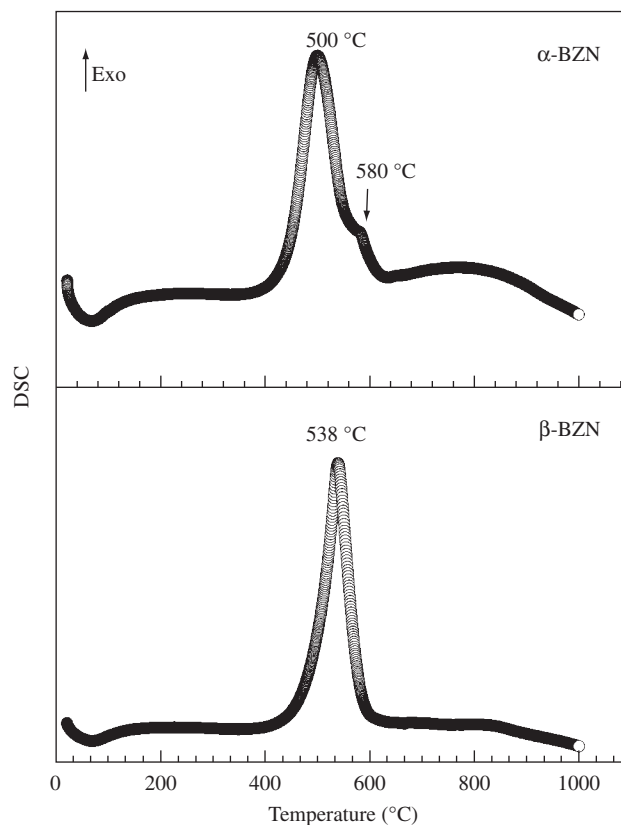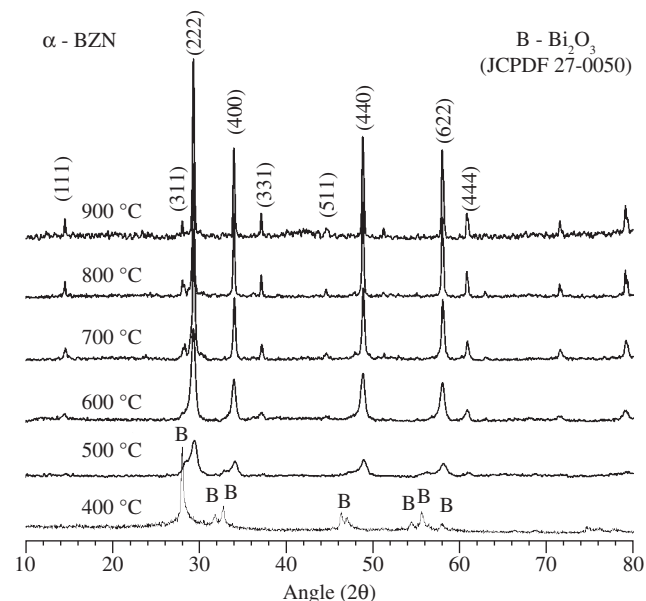**Figure 1.** Thermal analysis of BZN powders treated at 400 °C for 4 hours.

Figure 2. XRD patterns of α-BZN powders treated for 2 hours at temperatures ranging from 400 to 900 °C.

of Bi_2O_3 phase (JCPDS PDF 27-0050) was observed, nonetheless, at 500 °C the pyrochlore phase is already formed and coexists with Bi_2O_3 reminiscent; at 600 °C the pyrochlore peaks are somewhat broad indicating small and disordered crystallites. As expected, the increase of the annealing temperature to 700 °C leads to an increase in the degree of crystallinity of the samples.

Similar studies for α-BZN prepared by solid state reaction report that pyrochlore phase crystallizes through the formation of an intermediary $BiNbO_4$ phase. Bi and Nb cations react to form the $BiNbO_4$ compound at low temperatures, and the pyrochlore phase formation occurs through the reaction of $BiNbO_4$ and $ZnO^{9,11}$. In this study, no detectable intermediary phases, such as $BiNbO_4$, $Bi_5Nb_3O_{15}$ or pseudo-orthorhombic pyrochlore phase were ever observed in α-BZN composition. This result indicates that chemical synthesis conferred a higher chemical homogeneity and reactivity to the powder, leading to a different crystallization mechanism of the pyrochlore[18].

On the other hand, for the β-BZN composition, the Bi_2O_3 phase at 400 °C was also observed; nonetheless the crystallization mechanism is not the same. At 500 °C, the cubic phase (α-BZN) and $BiNbO_4$ (JCPDS 16-0295) intermediary phases, which coexist with the Bi_2O_3 reminiscent, are observed. These intermediary phases are evidenced at 600 °C. At 700 °C, the main peaks of the pyrochlore phase can be observed in coexistence with the unknown phase that remains even for the powder treated at 900 °C, as showed in Figures 3a and 3b. For pellets treated at 900 and 1000 °C for 2 hours, only the pyrochlore phase is present, while traces of an unknown phase can be observed for pellet sintered at 800 °C (Figure 3c).

The crystallite sizes for BZN powders were calculated from the diffraction data through the Scherrer´s equation:

$$D = \frac{0.9\lambda}{(\sqrt{b_{sp}^2 - b_{st}^2})\cos\theta} \tag{1}$$

where b_{sp} is the full-width at half-maximum (FWHM) of (222) and (221) diffraction peaks for α- and β-BZN, respectively; b_{st} is the FWHM for Si standard; θ is the Bragg angle, and λ is the CuKα wavelength (1.5428 Å). The crystallite sizes as a function of the temperature of thermal treatment are displayed in Figure 4 and ranged from 16 to 60 nm at temperatures ranging from 600 to 900 °C. It can be observed that the composition β-BZN presents smaller crystallites than those of α-BZN at the same temperature.

Figure 5a shows the FT-IR spectra for α- and β-BZN powders heated at 500 °C. No significant difference was observed in both spectra, where the bands related to O-H stretching modes and CH stretching modes, at 3437 and 2920 cm^{-1}, respectively, are observed. In the region from 2000 to 1500 cm^{-1}, the band around 1640 cm^{-1} is related to the OH stretching mode. Between 1500 and 1200 cm^{-1}, one can observe the bands at 1498, 1380 (carboxyl group stretching modes), and 1280 cm^{-1} (CO stretching modes). At lower wavenumbers several bands characteristic of the oxygen-metals/stretching mode, 645 and 523 cm^{-1} (for β-BZN), and 595 cm^{-1} (for α-BZN) are present[19,20].

Similarly, the Raman spectra (Figure 5b) of powders treated at 700 °C presented no huge difference for both compositions except for the intensities and for the band at 845 cm^{-1}, observed only for β-BZN composition. As expected, some extra bands can also be observed for the β-BZN composition due to the lowering of symmetry. The broadness of the features, probably due to nanometric particles, prevents an accurate estimation of the precise band frequencies. Reported bands for BZN pyrochlore[12] are located at 139, 195, 251, 271, 337, 369, 537, 623, and 764 cm^{-1}. The band at 251 cm^{-1} was assigned to Zn-O stretching mode while bands at 195 and 764 cm^{-1} correspond to Bi-O and Nb-O stretching modes, respectively.

The particle size of the powders treated at 700 °C, calculated from the surface area measured by N_2 adsorption/desorption isotherms

(a)

(b)

(c)
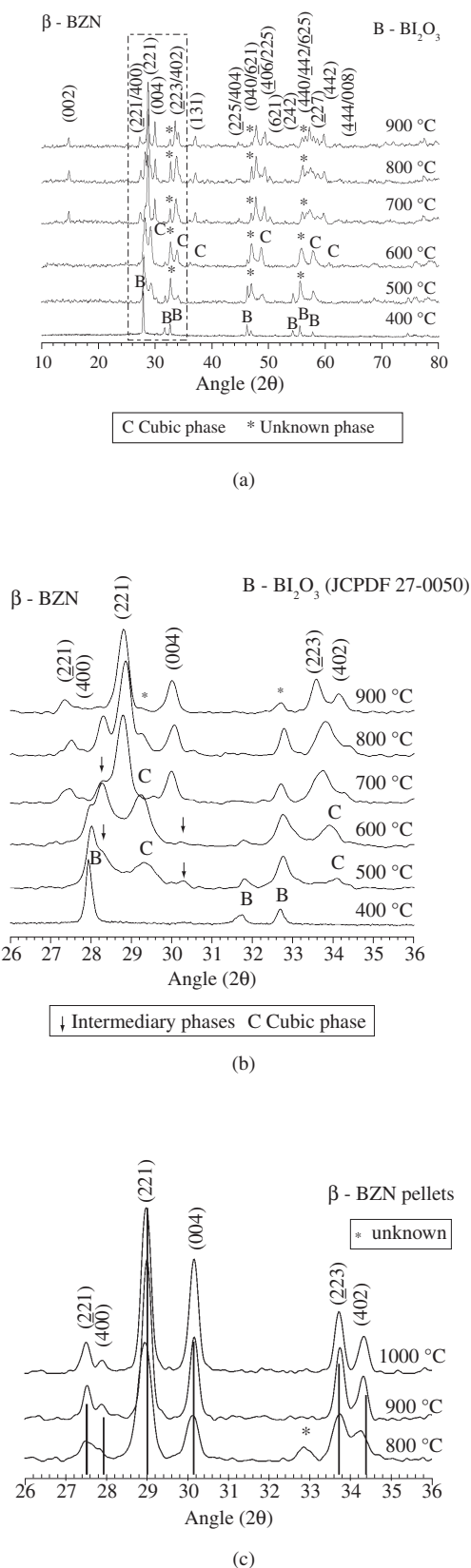
Figure 3. a) Extended XRD patterns of β-BZN powders treated for 2 hours at temperatures ranging from 500 to 900 °C; b) Zoomed 2θ range (26-36°) for powders; c) Zoomed 2θ range (26-36°) for pellets sintered from 800 to 1000 °C. (↓) denotes intermediary phases; and *denotes unknown phase.
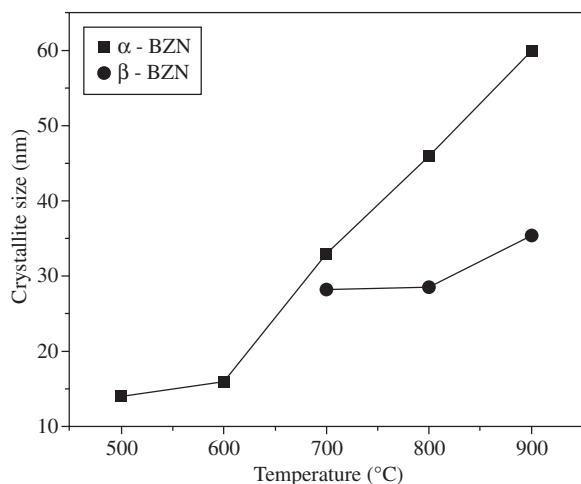
Figure 4. Crystallite size as a function of temperature for α-BZN and β-BZN powders.
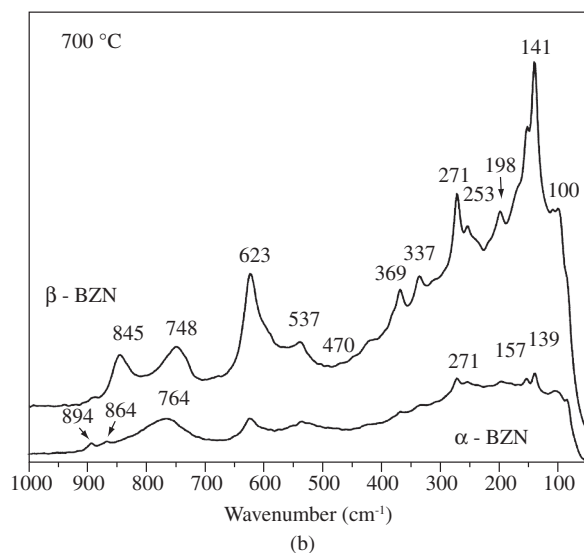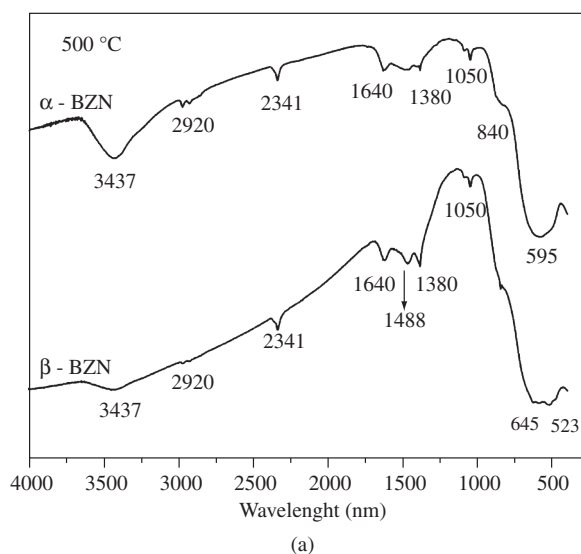
Figure 5. Spectra for α- and β-BZN powders heated at 500 and 700 °C, respectively. a) FT-IR; and b) Raman.

(BET), was 108 nm (7.8 m².g⁻¹) and 167 nm (4.6 m².g⁻¹), for α- and β-BZN, respectively.

The particle morphology observed by SEM and TEM is shown in Figure 6. The samples are formed by large agglomerated clusters with dimension in order of hundred nanometers. These agglomerated clusters are originated from the sintering of nanometer-sized particles during the thermal treatment. TEM images reveal the dimensions of the primary particles of around 50-100 nm for both compositions. These results are in agreement with the BET analysis.

The particle size distribution for both as-obtained compositions, measured by LALLS (Figure 7), showed a multimodal distribution with an average grain size ranging from 0.60 to around 30 μm which are formed basically by small and big aggregates. These results are in agreement with SEM observations.

Figure 8 shows the dilatometric analysis of pellets prepared with powder treated at 700 °C for 2 hours. The relative green density was 52.8 and 55.0%, for α-BZN and β-BZN, respectively. It can be observed that the maximum retraction rate occurs at 850 °C for both compositions.

The evolution of the apparent relative density (Archimedes method) as a function of the sintering temperature, displayed in Figure 9, reveals that the maximum relative density was reached at 800 °C (97.3%), for α-BZN (ρ_T = 7.11 g.cm⁻³), and at 900 °C (91.8%), for β-BZN (ρ_T = 7.94 g.cm⁻³). For temperatures above those, the apparent density decreased for both compositions, probably due to the extreme increase in the grain size accompanied by the increase in closed pore size,, which hinders the sample densification.

Figure 10 shows the microstructure of pellets sintered at 900 °C for 2 hours, in which a very porous microstructure was revealed. These porous microstructures are derived from the starting as-synthesized powders, with an unfavorable particle size distribution and aggregates.
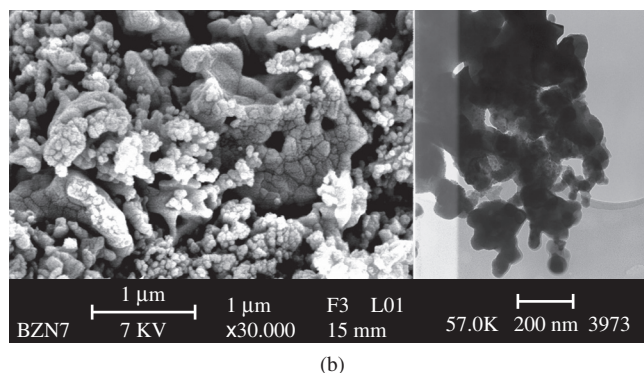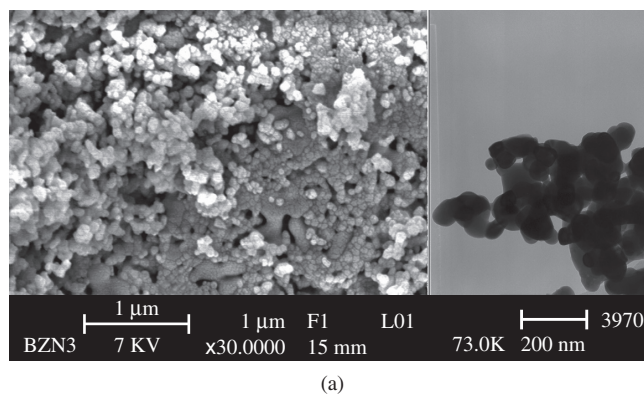
Figure 6. SEM and TEM images of powders treated for 2 hours at 700 °C: a) α-BZN; and b) β-BZN.

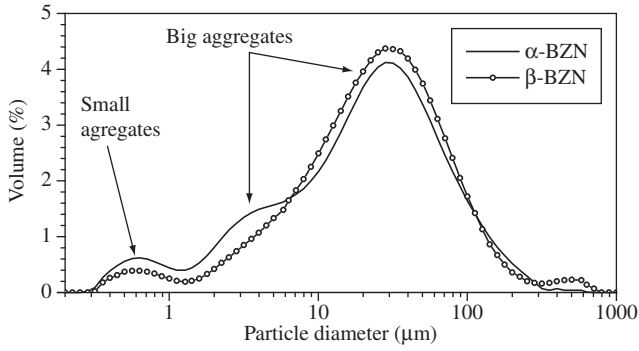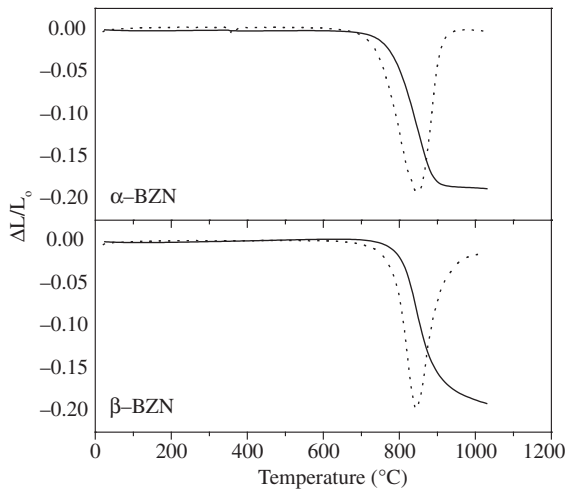**Figure 7.** Histogram of particles and aggregates size of BZN samples.

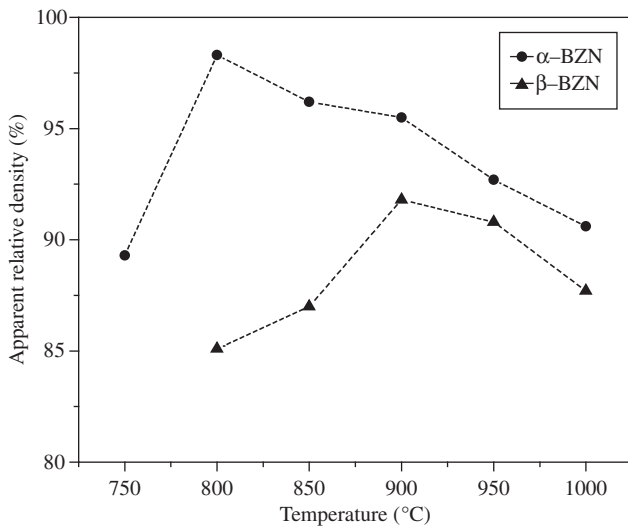**Figure 8.** Dilatometric analysis of α-BZN and β-BZN powders treated for 2 hours at 700 °C.

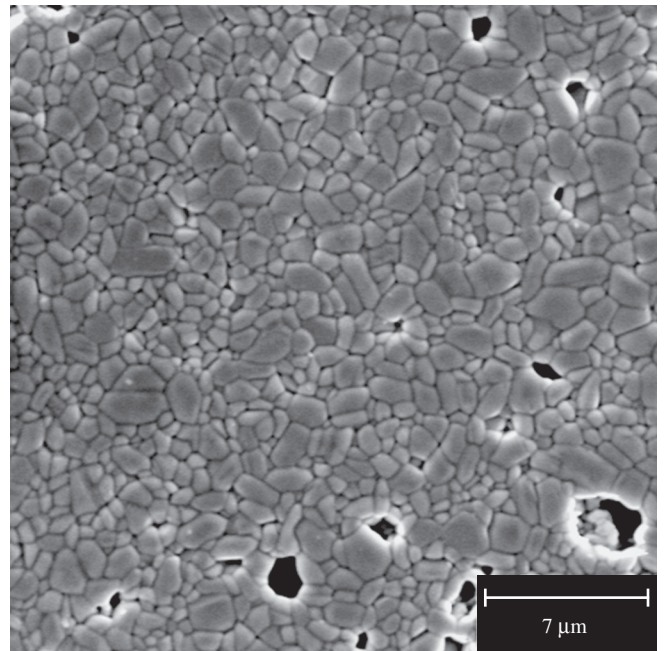**Figure 9.** Evolution of apparent relative density of α-BZN and β-BZN powders as a function of temperature.

For α-BZN sintered at 900 °C, a microstructure with grains larger than 7 μm (generated from the coalescence of the particles of the agglomerated clusters) mixed with smaller grains is observed. As
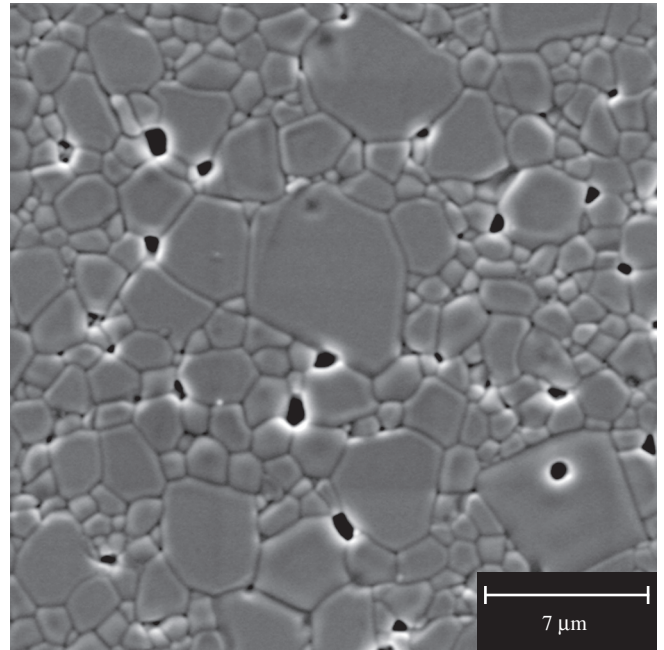
(a)

(b)

Figure 10. Microstructure observed by SEM of pellets sintered at 900 °C for 2 hours: a) α-BZN; and b) β-BZN.

the temperature increased the grains as well as the pore size became bigger due to the closed pores formed in the aggregates, mainly for α-BZN. It can be observed that β-BZN pellets also present a heterogeneous microstructure of elongated grains with different sizes that grew as the temperature increased. For β-BZN the grains are always smaller compared to those of α-BZN at the same temperature.

Electrical characterizations of pellets sintered at 900 °C were carried out at room temperature. Dielectric constant and dielectric loss,

at 1 MHz frequency, were 150 and 4 x 10^{-4} for α-BZN, and 97 and 8 x 10^{-4} for β-BZN. These results are similar to those reported for BZN pellets sintered at higher temperatures[11, 21].

4. Conclusions

Bismuth zinc niobate pyrochlores $Bi_{1.5}ZnNb_{1.5}O_7$ (α-BZN), and $Bi_2(Zn_{1/3}Nb_{2/3})_2O_7$ (β-BZN) were synthesized by chemical method based on the polymeric precursors. The study of α-BZN phase formation reveals that a single-phased nanopowder was obtained after calcination at 700 °C. No intermediary phase (as those reported for solid state reaction) was observed, indicating that the chemical method conferred a high chemical homogeneity to the powder. On the other hand, the β-BZN phase crystallizes through intermediary phases formed by cubic α-BZN and $BiNbO_4$. The α-BZN pellets, sintered at 800 °C for 2 hours presented a relative density of 97.3% while for β-BZN sintered at 900 °C for 2 hours it reached 91.8%. Dielectric constant and dielectric loss, measured at 1 MHz for pellets sintered at 900 °C for 2 hours, were 150 and 4 x 10^{-4} for α-BZN, and 8 x 10^{-4} for β-BZN, respectively. These results are similar to those reported for BZN pellets sintered at higher temperatures.

Acknowledgments

References

1. Vanderah TA. Talking Ceramics. *Science*. 2002; 298:1182-1184.

2. Bianco A, Gusmano G, Freer R, Smith P. Zirconium titanate microwave dielectrics prepared via polymeric precursor route. *Journal of the European Ceramic Society*. 1999; 19:959-963.

3. Kim JS, Kim JW, Cheon CI, Kim YS, Nahm S, Byun JD. Effect of chemical element doping and sintering atmosphere on the microwave dielectric properties of barium zinc tantalates. *Journal of the European Ceramic Society*. 2001; 21:2599-2604.

4. Su B, Button TW. The processing and properties of barium strontium titanate thick films for use in frequency agile microwave circuit applications. *Journal of the European Ceramic Society*. 2001; 21:2641-2645.

5. Kishi H, Mizuno Y, Chazono H. Base-Metal Electrode-Multilayer Ceramic Capacitors: Past, Present and Future Perspectives. *Japanese Journal of Applied Physics*. 2003; 42:1-15.

6. Valant M, Davies PK. Synthesis and dielectric properties of pyrochlore solid solutions in the Bi_2O_3-ZnO-Nb_2O_5-TiO_2 system. *Journal of Materials Science*. 1999; 34:5437-5442.

7. Levin I, Amos TG, Nino JC, Vanderah TA, Randall CA, Lanagan MT. Structural Study of an Unusual Cubic Pyrochlore $Bi_{1.5}Zn_{0.92}Nb_{1.5}O_{6.92}$. *Journal of Solid State Chemistry*. 2002; 168:69-75.

8. Wei J, Zhang L, Yao X. Melting Properties of Bi_2O_3-ZnO-Nb_2O_5-Based Dielectric Ceramics. *Journal of the American Ceramic Society*. 1999; 82(9):2551-2552.

9. Choi GK, Kim DW, Cho SY, Hong KS. Influence of V_2O_5 substitutions to $Bi_2(Zn_{1/3}Nb_{2/3})_2O_7$ pyrochlore on sintering temperature and dielectric properties. *Ceramics International*. 2004; 30:1187-1190.

10. Chen SY, Lee SY, Lin Y.J. Phase transformation, reaction kinetics and microwave characteristics of Bi_2O_3–ZnO–Nb_2O_5 ceramics. *Journal of the European Ceramic Society*. 2003; 23: 873-881.

11. Wang X, Wang H, Yao X. Structures, Phase Transformations, and Dielectric Properties of Pyrochlores Containing Bismuth. *Journal of the American Ceramic Society*. 1997; 80(10):2745-2748.

12. Wang H, Du HL, Yao X. Structural study of Bi_2O_3-ZnO-Nb_2O_5 based pyrochlores. *Materials Science and Engeneering B*. 2003; 99:20-24.

13. Wang H, Elsebrock R, Schneller RT, Waser R, Yao X. Bismuth zinc niobate ($Bi_{1.5}ZnNb_{1.5}O_7$) ceramics derived from metallo-organic decomposition precursor solution. *Solid State Communications*. 2004; 132:481-486.

14. Pechini MP. Method of preparing lead and alkaline earth titanates and niobates and coating method using the same to form a capacitor. US Patent 3.330.697. 1967 July 11.

15. Zanetti SM, Leite ER, Longo E, Varela JA. $SrBi_2Nb_2O_9$ Thin films deposited by dip coating using aqueous solution. *Journal of the European Ceramic Society*.1999; 19:1409-1412.

16. Zanetti SM, Leite ER, Longo E, Araújo EB, Chiquito AJ, Eiras JA, et al. An alternative chemical route for synthesis of $SrBi_2Ta_2O_9$ thin films *Journal of Materials Research*. 2000; 15:2091-2095.

17. Paris EC, Leite ER, Longo E, Varela JA. Synthesis of $PbTiO_3$ by use of polymeric precursors. *Materials Letters*. 1998; 37:1-5.

18. Zanetti SM, Silva SA, Thim GP. A chemical route for the synthesis of cubic bismuth zinc niobate pyrochlore nanopowders. *Journal of Solid State Chemistry*. 2004; 177:4546-4551.

19. Du H, Yao X, Zhang L. Structure, IR spectra and dielectric properties of Bi_2O_3–ZnO–SnO_2–Nb_2O_5 quarternary pyrochlore. *Ceramics International*. 2002; 28:231-234.

20. Nino JC, Lanagan, M T Randall CA, Kamba S. Correlation between infrared phonon modes and dielectric relaxation in Bi_2O_3–ZnO–Nb_2O_5 cubic pyrochlore. *Applied Physics Letters*. 2002; 81(23):4404-4406.

21. Du H, Yao X. Effects of Sr substitution on dielectric characteristics in $Bi_{1.5}ZnNb_{1.5}O_7$ ceramics. *Materials Science and Engeneering B*. 2003; 99:437-440.